

Novel aspects of confined organic systems

A Datta* and S Chattopadhyay

Surface Physics Division, Saha Institute of Nuclear Physics,
1/AF Bidhan Nagar, Kolkata-700 064, India

Abstract Confined organic systems such as ultra-thin polymer films exhibit structures and properties that are distinct from bulk organic materials. Au nanoparticles grown by sputter deposition in polystyrene films spin-coated on quartz and glass substrates have been studied using grazing incidence X-ray reflectivity and UV-visible spectroscopy. The nanoparticles are seen to form on top of the polymer film and they exhibit a transition in shape from spherical to ellipsoidal when the film thickness is decreased below $10 R_g$, R_g being the radius of gyration of the polymer. This result correlate with formation of layers and partial dewetting of substrates previously observed in strongly confined polymers.

Keywords . Shape transition, polystyrene, Au nanoparticles, confinement, X-ray scattering, UV-Vis spectroscopy

PACS Nos. 78.67.Bf, 78.70.Ck, 82.35.Np

1. Introduction

When some material is confined in one or more dimensions to within a length-scale of the order of some intrinsic size of the material (such as, for example, the molecular size) many novel properties of the material that are fundamentally different from the bulk are manifested [1]. Structurally the most significant aspect is the emergence of order due to confinement in materials that are disordered in bulk under the same ambient conditions. For confinement along one dimension this leads to layer formation normal to the direction of confinement. In recent years many computational, theoretical and experimental investigations have been carried out [2] to understand layer formation in liquids and polymer melts. Liquids in the form of thin films play a crucial role in a wide variety of phenomena. There is clear evidence that many physical properties [3] of confined liquids are different from those of the same liquid in bulk and the structure of liquids is modified when they are close to interfaces [4]. In other words, a confined liquid may no longer be a liquid.

One-dimensional confinement can be due broadly to two mechanisms. In the first, the interactions at the confining interfaces are very short range but very strongly repulsive, *e.g.* the 'ideally hard wall' interactions on an ultra-thin film, freestanding or on a 'non-interacting' substrate. This is the so-called *geometrical confinement*. The other form of confinement takes place when there is a specific attractive interaction which

itself is localized at some interface. A very good example of this is an amphiphilic molecule at the air-water interface. The attraction of one part (headgroup) and repulsion of the other part (hydrocarbon chain) of the molecule for water causes the formation of a monomolecular layer – the Langmuir monolayer [5]. These monolayers are known to form two-dimensional lattices with crystalline and liquid crystalline phases. The structures of these monolayers change with surface pressure, temperature [6], and pH of the water and presence of a particular dissolved metal ion [7].

Both types of confinement can exert strong effects on the properties of the films themselves as well as on structure and properties of materials such as nanoparticles grown in such films. Nanoparticles of metals such as Au, dispersed in a polymer, such as polystyrene, which does not wet them, can act as highly scattering monitors of X-rays to study polymer morphology [8]. Conversely, in-plane morphology of a polymer film may change with geometrical confinement as the film thickness is gradually decreased [9] and this may cause shape changes in any embedded nanoparticles.

Clear signature of layering has been observed in the electron density profile (EDP) of polystyrene (PS) spin-coated on Si(001), with the layering period close to twice the radius of gyration (R_g) of this PS, from grazing incidence X-ray reflectivity (GIXR) studies [10]. Polymers have a tendency to form nearly spherical coils [11] inside the solvent used to deposit thin polymer films

*Corresponding Author

by spin coating. The average radius of these coils is R_g , given by $r_0(M_w/6M)^{1/2}$, where r_0 is the unperturbed mean squared end-to-end length of the polymer, obtained from number of monomers and the length of each monomer unit, and M and M_w are number averaged and mass averaged molecular weights of the polymer [12]. It has been shown that polystyrene in coiled state exhibit Lennard-Jones (L-J) type potential [13]. The GIXR study indicates the formation of layers when these polymer 'balls' are confined geometrically between the smooth polymer-air and polymer-silicon interfaces [10]. This layer formation was observed in a film of thickness about $6 R_g$ whereas a film of thickness close to $9 R_g$ did not show any such layering. Similar layering was observed in confined liquid films with the layering period coinciding with molecular size and the layer amplitude decreasing with interfacial roughness [4].

In earlier X-ray scattering studies [9], it was also shown that although thick polymer films behave like liquid films, polymer films undergo de-wetting transition and micro-droplets are formed, when the thickness of the film becomes less than that of the radius of gyration of the polymer. Also from detailed studies

on non-wetting polybromostyrene/polystyrene bilayers it was observed that the top layer of polybromostyrene undergoes fragmentation and shape changes with changes in its thickness and the thickness of the underlying polystyrene layer [14].

These results, along with the fact that layer formation in polymer films starts only below a certain thickness (a particular multiple of R_g), prompted us to study the shapes, sizes and structures of Au nanoparticles grown in a non-wetting polymer (polystyrene) film. Here we present a spectroscopic and X-ray scattering study of shape transitions of Au nanoparticles sputter-deposited on spin coated polystyrene films. We are interested, in particular, in the situation when the thickness is around $1 R_g$.

2. Experiment and results

PS ($M_w = 560900$, $R_g = 215 \text{ \AA}$) films were prepared by spin coating on quartz and glass substrates from toluene solutions. The nominal thickness of the films was varied from $\sim 1 R_g$ to $\sim 11 R_g$ by changing the concentration of the solution and the angular velocity, using a calibration curve obtained previously. Au was sputtered on PS films of different thickness using a Pfeiffer

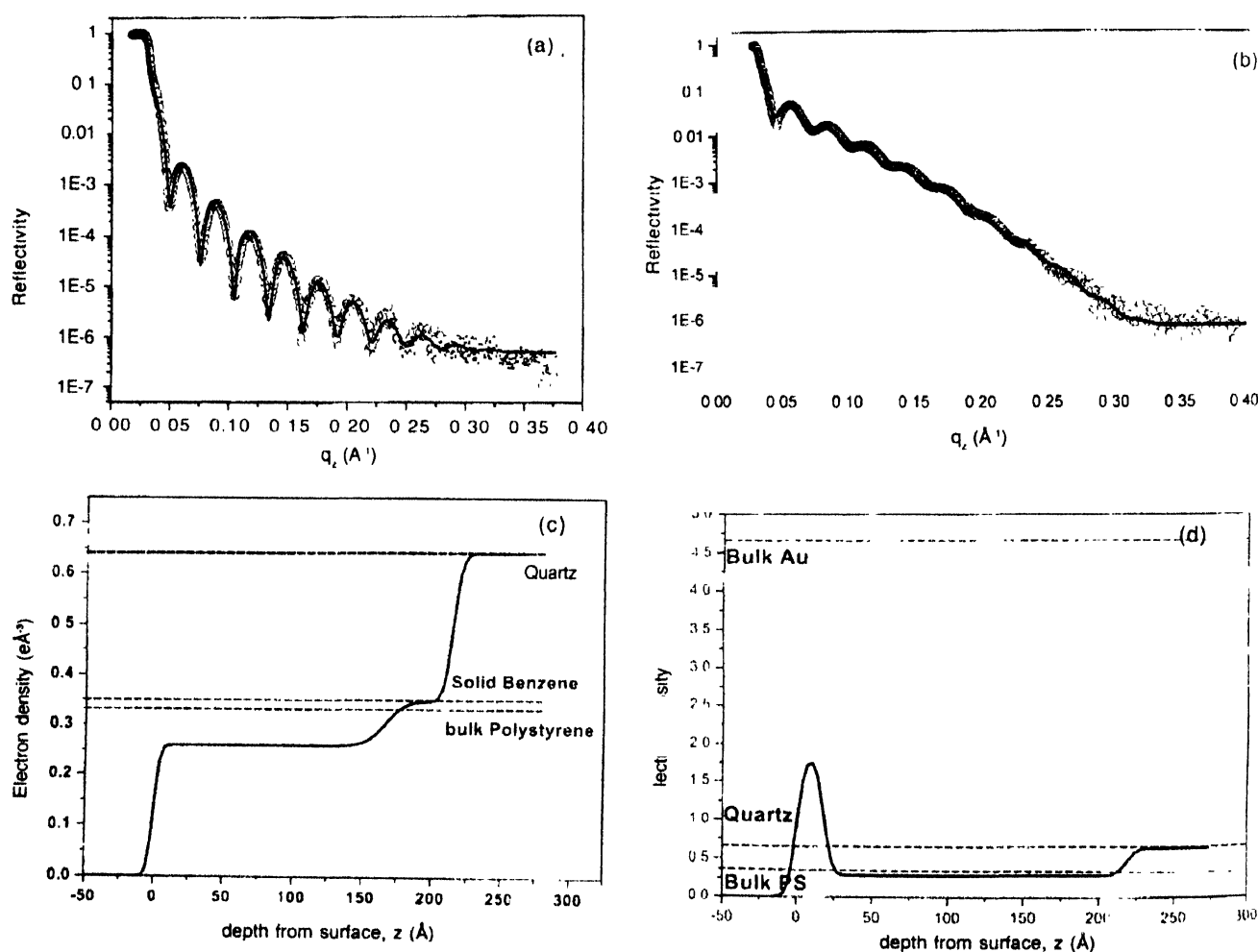


Figure 1. X-ray reflectivity versus q_z , the normal component of momentum transfer, i.e., X-ray reflectivity profile of (a) pristine PS film (thickness $\sim 1 R_g$) on glass and (b) Au-sputtered $1 R_g$ thick PS film on quartz. The continuous line is the fit to the data (in open circles) using standard formalism. The extracted electron density profiles (EDPs) of the respective films are shown in (c) and (d).

PLS500 DC magnetron for 5 s at 25 W (0.064A, 410V, 10sccm Ar gas flow, 4.7×10^{-3} mbar pressure). UV-visible spectra of the Au embedded films, always with a pristine film of same thickness as reference, were recorded in transmission mode in the 190–700 nm range using a GBC Cintra 10e spectrometer. An 18 kW rotating Cu-anode generator (Enraf Nonius FR 591) and Optix Microcontrol spectrometer was used to collect GIXR data 1 R_g thick films.

GIXR data for pristine and Au-sputtered nominally 1 R_g thick PS films on quartz are presented in Figures 1(a) and 1(b), respectively. None of these films show large roughness. Electron density profiles obtained from fits (continuous lines) using standard methods of analysis [4,10] are shown in Figures 1(c) and 1(d), respectively. The thickness of the pristine film is found to be ~ 215 Å, exactly matching the theoretical value of 1 R_g . From the EDP in Figure 2(c), the pristine film is seen to have no density variation, but to have about 70% of the density of bulk PS, consistent with partial de-wetting of the substrate by PS [9]. The layer of comparatively higher density adjacent to the

substrate is probably an indication of benzene rings in the polystyrene film taking up an average alignment parallel to the substrate, as has been predicted from contact-angle measurements [15].

The EDP in Figure 1(d) shows that the sputtered Au is almost entirely on top of the PS film. In presence of the high scattering density of Au, the reflectivity profile is comparatively insensitive to finer variations in density in the PS film and hence features such as benzene concentration are not detectable in this EDP. The low ($\sim 40\%$) coverage of Au indicates the formation of Au 'islands' or nanoparticles on top of the PS film. The slightly higher ($\sim 87\%$) coverage of the PS underneath is probably indicative of some diffusion of Au into the polymer.

Figure 2(a) shows the visible absorption spectrum of Au-sputtered 1 R_g polystyrene film. The peak in the visible region (~ 500 nm) is a clear indication of Au nanoparticles-formation [16]. Nanoparticles sizes were found using $\Gamma = 2\nu_F / d$, where Γ is full width at half maximum (FWHM) of the peak, ν_F is Fermi velocity of Au and d is the diameter of the Au nanoparticles [17]. Measurements were carried out to determine d as a function of PS film thickness. It was found that the average diameter, d_{av} of the Au nanoparticles showed a sudden but small increase from 30 Å to 48 Å when the PS thickness was reduced below 10 R_g (Figure 2(b)).

However, it was also observed (Figure 2(a)) that below this thickness of the PS film the visible spectrum of Au nanoparticles shows two peaks. This corresponds to two radii for each particle, indicating an ellipsoidal shape of the Au nanoparticles with ellipticity $\epsilon = a/b$ (a being the major radius and b the minor

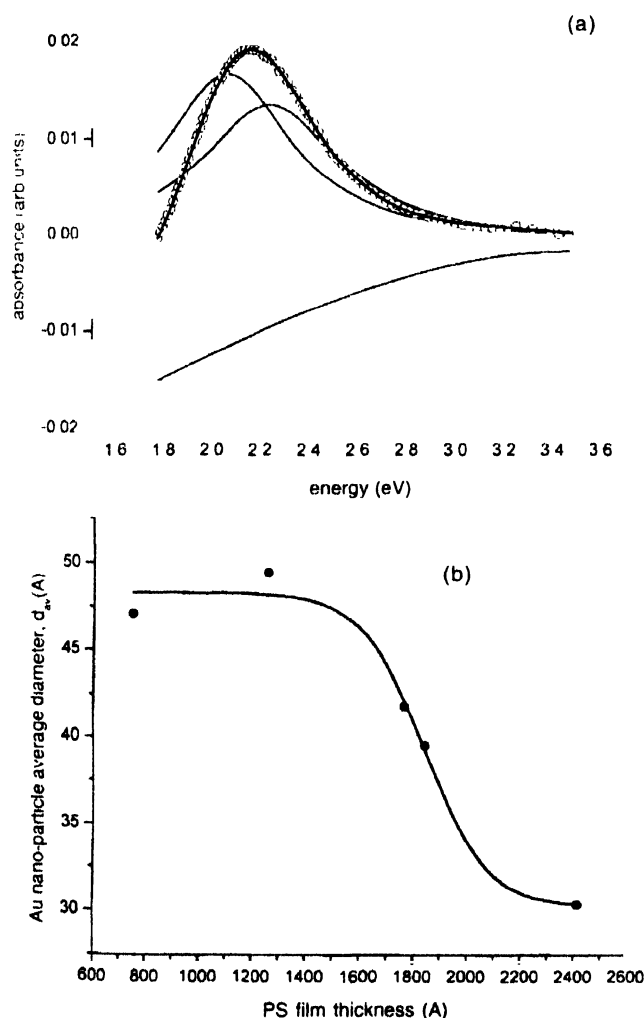


Figure 2. (a) Visible transmission spectrum of Au-sputtered 1 R_g thick PS film on glass. The two peaks corresponding to the two radii are shown. The third very broad peak at the high energy side is due to PS. (b) Average diameter d_{av} of Au nanoparticles versus PS film thickness on quartz.

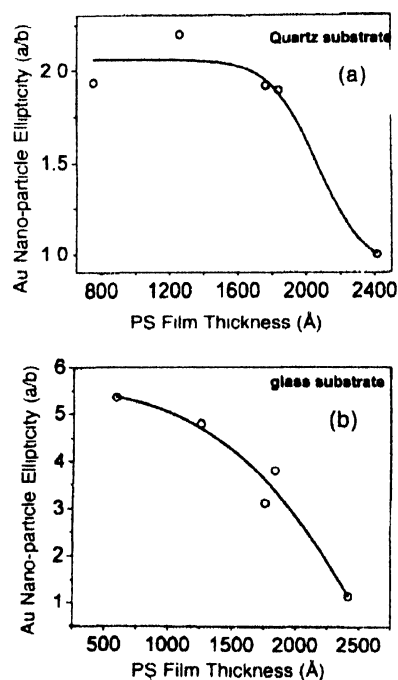


Figure 3. Ellipticity $\epsilon = a/b$, a = major radius and b = minor radius of Au nanoparticles versus PS film thickness on (a) quartz and (b) glass

radius) in the confined polystyrene matrix [16,18]. Plots of ϵ as a function of PS film thickness, with the PS coated on quartz (Figure 3(a)) and on glass (Figure 3(b)) are direct proofs of a shape transition of Au nanoparticles from spherical to ellipsoidal as the PS film decreases in thickness. This shape transition of deposited Au nanoparticles with decreasing thickness of the underlying polymer layer is an indication of the effects of repulsive forces between Au and PS under morphological changes in the PS film due to progressive confinement. Above a certain thickness ($\sim 9 R_g$), the polymer film is composed essentially of disordered gyration spheres, resulting in a film of uniform density [10]. Au nanoparticles on this film then assume a spherical shape dictated by free energy minimization. As the PS film becomes thinner, layering of gyration spheres commences and the Au nanoparticles are formed in the intervening spaces on top, with some degree of anisotropy in their growth, resulting in formation of ellipsoidal particle [14].

3. Outlook

The preliminary results presented here constitute the beginning of a detailed study correlating shape changes in nanoparticles with changing morphology of templates under confinement. It is known that semiconductor and metallic nanoparticles, confined in specific matrices, assume shapes that correspond to specific *habits* or distributions of facets of the respective nanocrystals [16]. Often these habits are not found in the equilibrium or bulk phases. Nanoparticles with an ellipticity which is a function of template morphology, as observed by us, provide an exciting opportunity to study, using techniques of high resolution crystallography, the role of nanocrystal-polymer interaction in the growth and stability of different facets of these non-equilibrium crystalline phases.

References

- [1] F F So and S R Forrest *Phys. Rev. Lett.* **66** 2649 (1991)
- [2] J van Alsten and S Granick *Macromolecules* **23** 4856 (1990)
- [3] O M Magnussen, B M Ocko, M J Regan, K Penanen, P S Pershan and M Deutsch *Phys. Rev. Lett.* **74** 4444 (1995); M J Regan, E H Kawamoto, S Lee, P S Pershan, N Maskil, M Deutsch, O M Magnussen, B M Ocko and L E Berman *Phys. Rev. Lett.* **75** 2498 (1995)
- [4] C-J Yu, A G Richter, A Datta, M K Durbin and P Dutta *Phys. Rev. Lett.* **82** 2326 (1999)
- [5] I Langmuir *J. Am. Chem. Soc.* **39** 1848 (1917)
- [6] V M Kaganer, H Möhwald and P Dutta *Rev. Mod. Phys.* **71** 779 (1999)
- [7] J Kmetko, A Datta, G Evmenenko and P Dutta *J. Phys. Chem.* **B105** 10818 (2001)
- [8] Binhua Lin, T L Morkved, M Meron, Z Huang, P J Viceard, H M Jaeger, S M Williams, M L Schlossman *J. Appl. Phys.* **85** 3180 (1999)
- [9] W Zhao, X Zhao, M H Rafailovich, J Sokolov, L J Filters, R Plano, M K Sanyal, S K Sinha and B B Sauer *Phys. Rev. Lett.* **70** 1453 (1993)
- [10] M K Sanyal, J K Basu, A Datta and S Banerjee *Europhys. Lett.* **36** 265 (1996)
- [11] P G de Gennes *Simple Views on Condensed Matter Physics* (Singapore: World Scientific) (1992)
- [12] M Doi and S F Edwards *The Theory of Polymer Dynamics* (New York: Clarendon Press) (1988)
- [13] J Klein *Nature* **288** 248 (1980)
- [14] D Slep, J Asselta, M H Rafailovich, J Sokolov, D A Wmsett, A P Smith, H Ade and S Anders *Langmuir* **16** 2369 (2000)
- [15] O N Tretinnikov *Langmuir* **16** 2751 (2000)
- [16] C F Landes, S Link, M B Mohamed, B Nikoobakht and M A El Sayed *Pure Appl. Chem.* **74** 1675 (2002)
- [17] W P Halperin *Reviews of Modern Physics* **58** 533 (1986)
- [18] K L Kelly, E Coronado, L L Zhao and G C Schatz *J. Phys. Chem.* **B107** 668 (2003)